Article

The New Physics in LILITA_N21: An Improved Description of the Reaction 190 MeV ^{40}Ar + ^{27}Al

Antonio Di Nitto [1,2,*], Federico Davide [1,2], Emanuele Vardaci [1,2], Davide Bianco [2,3], Giovanni La Rana [1,2] and Daniela Mercogliano [1,2]

[1] Department of Physics "E. Pancini", University of Naples "Federico II", 80126 Naples, Italy; federicodavide2727@gmail.com (F.D.); vardaci@na.infn.it (E.V.); larana@na.infn.it (G.L.R.); da.mercogliano@studenti.unina.it (D.M.)

[2] National Institute of Nuclear Physics (INFN), 80126 Naples, Italy; d.bianco@cira.it

[3] Italian Aerospace Research Centre (CIRA), 81043 Capua, Italy

[*] Correspondence: adinitto@na.infn.it

Abstract: In this paper, light charged particle emission in the evaporation residue channel for the 190 MeV ^{40}Ar + ^{27}Al reaction leading to ^{67}Ga composite nuclei at E_x = 91 MeV and angular momentum up to 46 ħ has been re-analyzed. The main goal was to study the decay of ^{67}Ga on the basis of an extended set of observables in order to provide a description of the evaporative decay cascades using the multistep Monte Carlo approach. The proton and α-particle energy spectra along with their angular distributions and ratios of differential multiplicities have been considered. The measured observables were compared with statistical model calculations. Having used a single-step Monte Carlo approach and standard parameters decades ago, the model does not provide a good description of the full dataset. Only a subset of the data was reproduced by assuming emitting nuclei with very large deformed shapes in a previous work published in the late 1980s. In the reported analysis, better agreement has been observed. Using the new transmission coefficients from the Optical Model, the parameters of which have recently been derived, the multi-step approach and the introduction of a nuclear shape description based on the nuclear stratosphere allowed us to realize a significant improvement.

Keywords: fusion–evaporation reactions; statistical model; heavy ions; light charge particles

1. Introduction

Statistical models were created in the late 1940s to describe compound nucleus (CN) evaporative decay processes [1,2]. However, broader applications aimed at describing in more details the physical processes required the implementation of the Hartree–Fock theory, which overcomes the simple classical and geometrical arguments and introduces a proper quantum mechanical treatment of angular momentum [3]. These models, originally developed to describe the processes occurring at very low excitation energy, were later extended by increasing their complexity in order to take into account effects manifesting at higher excitation energy and angular momentum.

This model evolution corresponds to the chronological development of the subject driven by the use of accelerator facilities providing atomic nuclei beams at wide mass intervals spanning from Li up to U and at energies sufficient to overcome the Coulomb repulsion generated by target nuclei and to form excited nuclei through different reaction mechanisms.

The use of statistical theory was historically adopted to describe the compound nucleus decay that proceeds via a succession of intermediate states the evolution of which, beyond conservation laws, is unaffected by the entrance channel. Although this approach (based on the Bohr argument that sees the compound nucleus as a system that evolves through states in thermal equilibrium) is weak, it becomes less and less valid with the

increase of excitation energy when two or more particles can be emitted sequentially and the competition with fission decay takes place.

Thus, multi-step emission processes can be modeled by extending the basic formalism; the solution usually adopted consists in the construction of Monte Carlo event generators based on the theoretical statistical models. These implementations have the advantage of automatically considering the competitions and correlations among the particles emitted and the residual nuclei produced in multi-step processes. Nevertheless, variations of this model remain useful, especially at higher excitation energies. The success of statistical theories has led to the development of a number of sophisticated computer codes which are widely used for calculating nuclear evaporation properties such as neutron and charged-particle energy spectra, multiplicities, cross sections, residue velocities and yields, photon distributions, etc. As these codes are rapidly finding applications in uncharted areas, it is important to have a clear view of the weaknesses and potential difficulties of the basic model in order that we do not confuse new phenomena with old and perhaps unrecognized shortcomings.

The Statistical Model (SM), despite being a powerful tool, is not always able to reproduce the physical observables in an optimal manner. Numerous articles in the late 1980s and early 1990s highlighted gaps in its predictive power at extreme conditions such as high energy and angular momenta. In the case, for example, of hot nuclei, it is sometimes necessary to use different parameterizations to describe nuclear behavior well. For instance, good agreement between calculation results and experimental data can be achieved only by resorting to unrealistic parameterizations that do not ensure the simultaneous reproduction of all experimental observables. Therefore, a collection of a large dataset including many observables is needed in order to calculate the suitable parameters for different reactions. In general, the global failure of the model can be attributed to the lack of dynamics in describing the evolution of the excited system, suggesting the need for essential ingredients in the standard SM that can be investigated by reanalyzing the systems that show larger discrepancies.

Large discrepancies between experimental data and simulations for compound nuclei with mass number A = 150 have been evidenced in energy spectra, angular distributions, and multiplicities of neutrons, protons, and α-particles [4–10]. Although different modifications of the standard SM parameters have been considered, none of them permits simultaneous reproduction of the wide set of experimental observables available. These limitations can be ascribed to the incorrect treatment of the problem and to the competition with the fission channel. However, difficulties in reproducing the experimental data have been observed in the mass region around A = 60 at very high angular momenta, where the competition with the fission channel can be considered negligible. Examples include the 120 MeV ^{30}Si $+^{30}$ Si reaction [11], where the α-particle energy spectra were much softer than simulated ones, resulting in their being shifted at a higher energy with a significantly broader distribution, and the 190 MeV ^{40}Ar $+ ^{27}$Al [12] reaction, which is the subject of the present reanalysis. The global behaviour observed in these two systems was the reason for our invoking the need for new physics in the statistical model [12].

Several attempts to correct the standard SM and to return to satisfactory overall pictures for these extreme cases have failed. Often, they allowed correct reproduction of only one observable at a time. For instance, in the work of La Rana et al. [12], assuming emission from very deformed nuclei with a near-prolate shape, with ratios of major-to-minor axes of the deformed emitter up to 3, and with the reduction of the Coulomb barriers, it was possible to reproduce α-particle energy spectra and proton and α-particle multiplicities, though not the proton energy spectra. The lesson learned is that it is crucial to consider a large set of observables in order to avoid controversial conclusions. At present, a global solution is missing, although these limitations of the standard SM have been known for decades and the behaviour of reaction systems at high energy and spin represents a benchmark for studies of new frontiers. The introduction of the nuclear stratosphere model [13] is aimed at eliminating effects due to deformations and variations of the channel

competition at extreme angular momentum. In fact, the observed trends of the energy spectra and angular distributions can be related to the occupation of high-lying single-particle levels occurring with the increase of the nuclear temperature, which consequently changes the distribution of nuclear density. More generally, at high temperatures when the nucleus is more excited a balance between the density distribution decrease in the inner core and its increase in the surrounding stratosphere should be pursued. This balance is achieved by the contraction of the volume part and the expansion of that part of the surface employing high single-particle orbits. In this work, after a brief description of the recently-developed computer code LILITA_N21 [14], the reanalysis of the light charge particle observables collected in the 190 MeV ^{40}Ar + ^{27}Al [12] reaction and the SM ingredients used to describe the evaporative decay process are discussed.

2. Materials and Methods

The Model

Although several mechanisms favor barrier penetration in heavy-nuclei collisions with energies near to or below the Coulomb barrier, the typical fusion reaction realm is accessible at energies high enough to overcome the Coulomb barrier. The intermediate system produced is called a Compound Nucleus. A CN is characterized by excitation energies and angular momenta distributions depending on the kinematic conditions and the properties of colliding nuclei. Lifetimes larger than 10^{-20} s, that is, the characteristic time for a transition between compound nuclear states, assure the complete thermalization of the system's degrees of freedom and, according to Bohr's independence hypothesis, in the decay pattern there is no memory of the entrance channel. This system can rapidly decay through the emission of particles. The modeling of this process is essential to the comprehension and analysis of CN decay; therefore, the evaluation of the production cross sections, angular and energy particle distributions, and multiplicities of decay channels should be reproduced by models.

The description of the decay process needs to take into account the phase space available for the emitted particles and evaporation residues. With increasing excitation energy, the distance between accessible nuclear levels is reduced while their width increases, generating a continuum of the states. Hence, it is no longer possible to describe the decay process with the Breit–Wigner formula [15], although it remains convenient to introduce the concept of nuclear level density (NLD) and adopt a statistical treatment. This latter approach represents one of the most-used in the study of evaporative decay. Codes capable of simulating all the physical quantities listed above have been implemented using different computational methods, either of the analytical or Monte Carlo type, such as for instance CASCADE [16], HIVAP [17] and PACE [18,19], and LILITA [20].

In this approach, the features of decay cascades depend on the particle emission probabilities, thus, these quantities have to be calculated for different types of particles once considering all energies and angular momenta available and with respect to the detailed balance and Bohr's independence principles. Then, the calculations of the fusion evaporation products becomes possible by coupling these probabilities with the Monte Carlo method to determine the decay cascade for each event. More specifically, the code generates a series of events. Each event starts with the definition of the excited compound nucleus, the excitation energies, and the angular momentum taken from user-defined distributions, then the code proceeds by calculating the evaporative cascade. The decay consists of several steps; for each of them, the code calculates the mass, charge, excitation energy, and angular momentum of the evaporation residue and the kinematics of the emitted particle. The process stops when the energy of the evaporation residue is no longer sufficient to emit further particles. The advantage of Monte Carlo codes with respect to analytical ones depends on event-by-event calculations the results of which can be stored on files. By filtering these files, it is possible to extract the quantities of interest taking into account the response function of the measurement apparatus.

Among the leading parameters of the SM that affect emission probability, it is worth considering the following: the NLD "a" parameter, the value of which is provided by the Fermi Gas Model [21]; the Transmission Coefficient (TC), i.e., the probability for particles to be emitted, which is calculated through inverse reaction cross-section measurements using the reciprocity theorem (detailed balance) of nuclear reactions; and the nuclear shape of emitters. The NLD "a" parameters, originally extracted from the average spacing observed in slow neutron resonances [21], show large variations within a range from $a = A/13 \, \text{MeV}^{-1}$ [22] to $a = A/6 \, \text{MeV}^{-1}$ [7,23] and have been estimated in light systems by comparing experimental data collected in heavy-ion induced reactions to SM calculations. The most widely used TC are those based on the Optical Model (OM) potential parameters, usually dubbed OMTC. Several systematics for the different particles have been considered. Then, local [24–26] and global fits [27,28] can be performed to determine the Woods–Saxon potential parameters. The optical model parameters do not take into account nuclear deformations; hence, a nuclear matter density distributed according to the nuclear stratosphere model [13] has been considered and implemented to modulate the transmission coefficient parameters on the basis of the (h, b) parameters. The nuclear shapes affect the decay probability and enter into the calculations by means of the moment of inertia. The moment of inertia for spherical emitters depends on different values of the r_0 parameters considered, and can be modulated to take into account the nuclear elongation by means of deformability parameters. A commonly used ansatz (see for instance [6,29–31]) scales the moment of inertia with the angular momentum in order to consider deformations according to the rotating liquid drop model [32] or for super- and hyper-deformations. In order to consider the widest variability of these parameters in this paper, we used LILITA_N21 [14].

3. Results

In this section, a comparison between experimental data and simulations obtained with the LILITA_N21 code is presented. For the purpose of comparison, the two calculations described in the following section were considered. The aim was to reproduce the observables of the 190 MeV ^{40}Ar + ^{27}Al reaction forming ^{67}Ga compound nuclei at an excitation energy of about 91 MeV and angular momentum up to 46 ℏ. We considered this reaction because it represents a good test case for which high quality data that include proton and α-particle energy spectra and angular distributions are available. The authors of [11] evidenced the limitations of the standard statistical model implemented in the single-step Monte Carlo code GANES in simultaneously reproducing all the observables. A satisfying reproduction of the full set of observables was not obtained by assuming reduced barriers for the charge particles and deformations much larger than those expected for nuclei at large angular momentum (i.e., in the extreme region [33]), Ref. [12].

A peculiar parameter combination that reproduces only part of the reaction products cannot provide a good description of the CN; hence, we carried out a new analysis. The simulations here were performed with LILITA_N21, a multi-step Monte Carlo evaporative code into which the parameters shown in Table 1 were fed. As leading prescriptions in both calculations, a constant NLD "a" parameter ($a = A/8 \, \text{MeV}^{-1}$) and an OMTC from the newest systematics for neutrons, protons, and α particles [27,28] were adopted. The difference among the two calculations is the model describing the nuclear shape. In the first, we considered emitting nuclei with a spherical shape (SS) and an $r_0 = 1.2$ fm, whereas for the second we used the Nuclear Stratosphere (NS) model according to the parameterization given in [13].

Table 1. Input parameters for the LILITA_N21 simulations.

	NLD "a"	Nuclear Shape Parameters	TC
SS	A/8	r_0 = 1.2 fm	OM [27,28]
NS	A/8	(h, b) = (0.079, 0.7)	OM [27,28]

3.1. Light Charged Particle Spectra

The energy and angular distributions and the abundance of evaporative LCP emission can provide important information concerning the statistical properties of hot rapidly-rotating nuclei. In particular the shape of the low-energy cutoff of evaporative spectra are controlled by the effective barrier (or its time-reversed capture process). Consequently, we can expect the spectra and angular distributions to reflect the role of effective emission barriers, which are associated with the sizes and shapes of emitters. In an attempt to refine the description of the relevant potential barrier between cold nuclei, the fusion data available in 1980s paved the way for the development of transmission coefficients from fusion systematics, replacing the existing ones extracted in the 1970s which considered only elastic scattering data. Transmission coefficients built by considering only fusion cross sections were later implemented in the GANES code and used to analyze the reaction under study here [12]. In the work by L. C. Vaz and J. M. Alexander [34], only fusion barriers of light charged particles were considered, while it is known that strong competition between protons and neutrons emission exists. This is probably one of the reasons explaining why GANES code does not reproduce the proton spectra even when by assuming a large deformation [12].

On the basis of these considerations, we implemented in our code the global OM parameters taken from [27]. The potential parameters were derived by considering: (i) a dataset including different observables from both non-elastic and elastic scattering data; (ii) a reliable competition between the neutron and proton emissions ensured by the use of the same functional form for protons and neutrons except for the Coulomb correction term. However, it is worth mentioning that OM parameters are extracted by fitting experimental data collected using target nuclei in their ground states; thus, deformations of the compound nuclei such as those predicted by the RLDM can modify the evaporation barrier. To extend the validity of our approach in a broad mass region we introduced the possibility of modulating our transmission coefficients calculated using the Optical Model potential by means of the Nuclear Stratosphere parameters.

In Figure 1, we show the proton and α-particle energy spectra from the evaporation channel. All the spectra are normalized to the maximum in order to show the differences. The experimental data and the GANES simulation results are taken from [12]. It can be seen in Figure 1 that the LILITA_N21 calculations reproduces both the low- and high-energy sides of the spectra. The better reproduction of the low-energy side can be ascribed to the adoption of the global OM parameters. All OM parameters used in the TC calculations are the result of global fits; however, it is worth mentioning that they were obtained with independent fits for protons and neutrons and for α particles, which were taken from [27,28], respectively. In terms of the fits, the elastic and inelastic angular distributions of light particles impinging at different energies on nuclei distributed over wide data mass intervals were considered. The use of these recent TCs allows for increasing the emission probability of low-energy light charge particles. It was not possible to obtain similar results for protons, even when including very deformed shapes for the emitting nuclei; see [12].

In our calculations, the NLD "a" parameter does not change as function of the particles and is kept equal to a $= A/8$ MeV^{-1}, i.e., we used the empirical value extracted from the average spacing observed in slow neutron resonances [21]. Therefore, the improvement in the high-energy sides of the spectra is very likely due to the greater reliability of the calculations obtained with a multi-step code that includes parameters from wider systematics.

The NS (h, b) parameters used in the calculations were obtained according the procedure described in [14], in which the proton and α particle spectra at 45° in the laboratory system were fitted. We considered the experimental spectra shapes available at the most backward direction, because these are usually less affected by particles originating in faster reactions. By introducing the NS combination, the slopes of α-particle at high energies are better reproduced. Although the introduction of this model produces small differences in the energy spectra, it is worth stressing that this is relevant for a general reproduction of the evaporative decay of CN as much larger effects are expected to occur for nuclei at larger angular momenta and mass; see for instance the calculations of ^{160}Yb in [14].
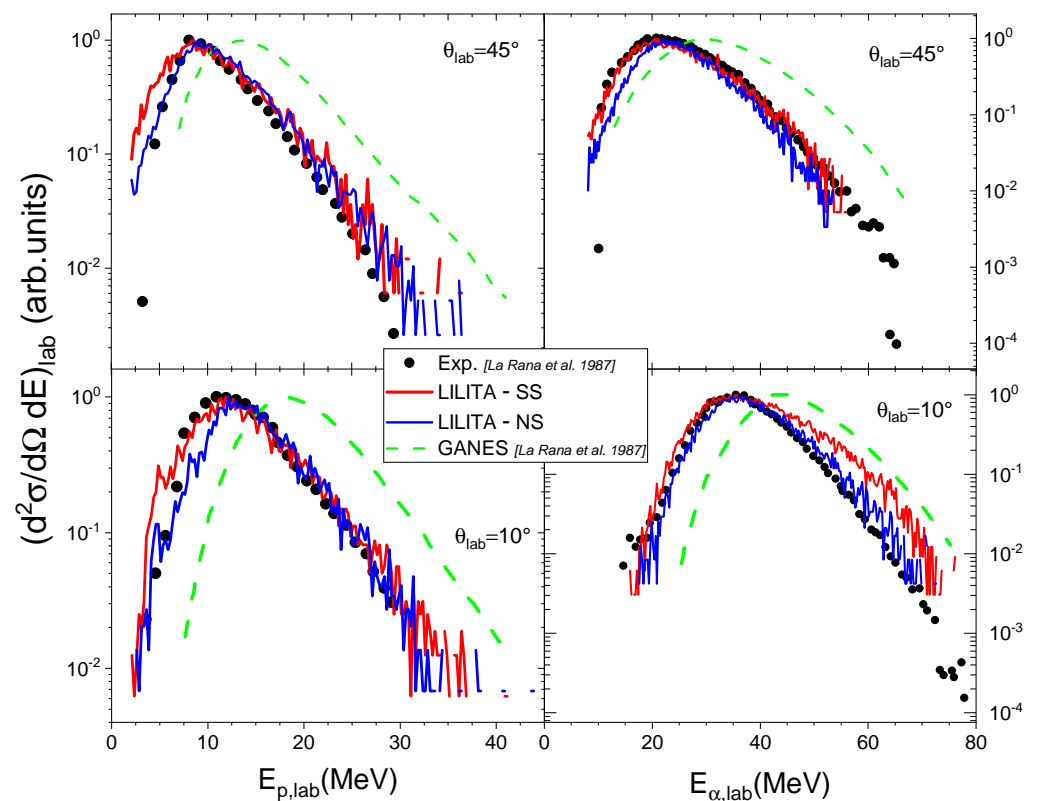
Figure 1. Proton and α-particle energy spectra. The experimental data (dots) from [12] are compared with LILITA_N21 calculations using the SS (solid red line) and NS (solid blue line) and the GANES calculations (dashed green line) assuming emission from spherical nuclei, data from [12]. For more details, see the text.

3.2. Angular Distributions

In Figure 2 the angular distributions of proton and α-particles in the center-of-mass system are compared with the calculations. The calculated distributions were normalized to the experimental data at the larger angle, i.e., the angles at around $\theta_{cm} = 90°$. This normalization was performed in order to better show the variation of the anisotropies due to the rotational energy and moment of inertia characterizing the compound nucleus at different stages of the evaporative cascades. The angular distributions obtained with LILITA_N21 simulations better reproduce the angular distributions of protons, while by using GANES the experimental data were not close to being reproduced assuming emission from spherical nuclei. Almost the same accuracy was obtained with both prescriptions. Instead, the alpha-particle angular distributions are slightly overestimated for the same amount, as observed with GANES.

Further improvements can be achieved by using a finer step in the calculation grid, optimized thus far only to reproduce the shape of energy spectra at a fixed laboratory angle. However, the main conclusions regarding the substantial improvements do not change, and the evident step forward can be ascribed to the better description of the system reached using the new OM transmission coefficients with a multi-step decay code.
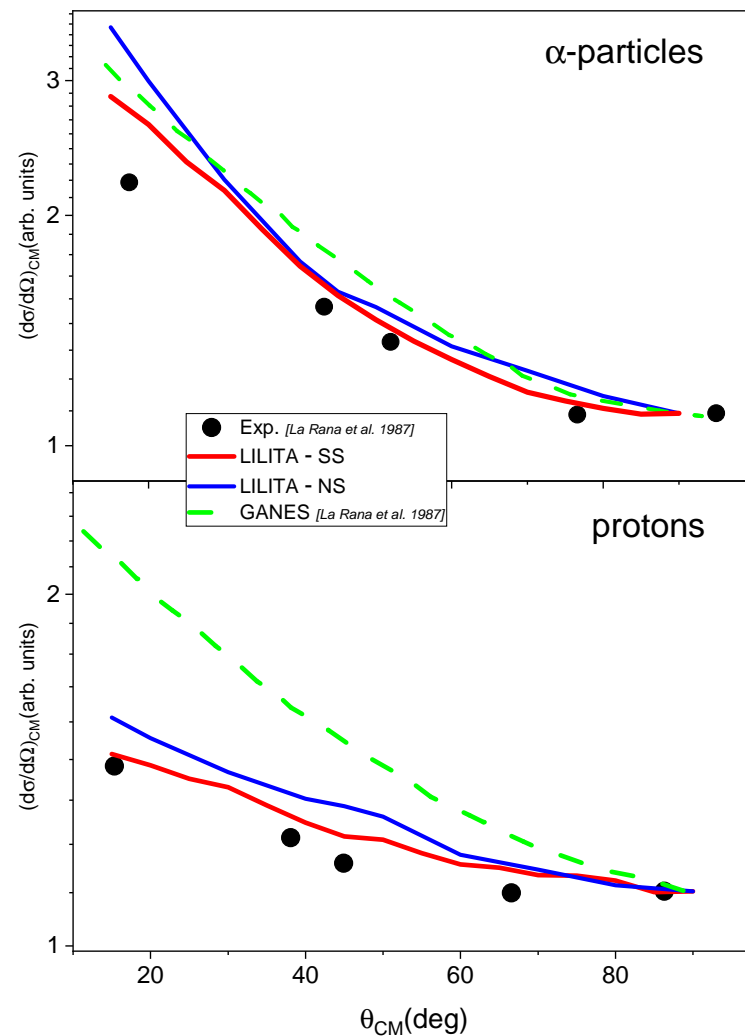
Figure 2. Angular distributions of α particles and protons in the center of mass system. The experimental data (dots) from [12] are compared with LILITA_N21 calculations using the SS (solid red line) and NS (solid blue line) and the GANES calculations (dashed green line) assuming emission from spherical nuclei, data from [12]. The calculated curves have been normalized to the data at around 90°. For more details, see the text.

3.3. Differential Multiplicities

It is well known that the NLD "a" parameter affects the shape of the energy spectra and is often extracted by fitting the simulated spectra onto the experimental data measured at different energies and by separately considering the different particle types [35,36]. However, it is worth noting that this leading parameter, in connection with the moment of inertia (calculated by taking into account the size and shape of emitting nuclei), strongly affects decay cascades by influencing particle emission competition. In other words, the final evaporation multiplicities depend on it; see for instance [23]. Thus, in order to further investigate the validity of the assumed NLD "a" parameter and the deformation contributions in our calculations, the differential multiplicity ratios between α particles and protons at different polar angles were considered. The energy spectra present in the paper do not allow us to extract the differential multiplicities at different angles because of the limited resolution of the figures and the variable binning sizes. Therefore, we considered the double differential multiplicities corresponding to the maximum of the spectra at different laboratory angles. In Table 2 the double differential multiplicity ratios among α particles and protons measured at the most forward and most backward directions are reported.

Table 2. Double differential multiplicities ratio among α particles and protons measured at most forward ($\theta_{lab} = 10°$) and most backward ($\theta_{lab} = 45°$) directions. The experimental data from the literature are compared with LILITA_N21 calculations using the SS and NS prescriptions. For more details, see the text.

θ	Exp. [12]	LILITA-SS	LILITA-NS
10°	1.56	2.04	1.62
45°	0.55	1.12	0.81

The experimental data were compared only with the LILITA_N21 simulations, as the maxima are quite well reproduced. The emission probability in the SM depends on the available energy, and therefore such a comparison makes sense only if ratios of differential multiplicities at the same energies are considered. Consequently, we did not include in the comparison the GANES calculations, as these show maxima at energies about 10 MeV larger than the experimental ones. The differences between the calculations and the experimental data range from 4–20% and 24–60% in the case of the NS and SS prescriptions, respectively. The large improvement observed by adopting the NS model is very interesting, as better reproduction of the experimental data was obtained for the spectra measured at $\theta_{lab} = 10°$, whereas the NS parameters were obtained by fitting the nuclear shapes at $\theta_{lab} = 45°$. Furthermore, these results should mainly be attributed to the general reliability of the code more than to the introduction of two free parameters fitted on the experimental data. In fact, none of the fitting procedures for the particle multiplicities were taken into account.

4. Discussion and Conclusions

In previous experiments, the description of the energy spectra of α-particles and protons emitted from nuclei produced at large angular momenta required resorting to very large deformations for high spin compound nucleus states [11,12] or required an ad hoc modification of the ingredients included in the SM, as for instance in [9,37]. The charged particles emitted in the evaporation channel in light composite systems make them well suited for verification of the evaporation decay process description provided by the statistical model. These particles are (i) very sensitive to the nuclear shapes of emitting nuclei, and (ii) originate by a single decay process dominating at all angular momenta, i.e., it is in negligible competition with other processes, such as fission. Hence, they represent powerful probes to map nuclear shape evolution as a function of excitation energy and angular momentum. In this work, we reanalyzed the evaporative light charged particles emitted by the ^{67}Ga nuclei at $E_x = 91$ MeV by performing a comparative analysis of data and GANES simulations from the literature [12] with the results of the LILITA_N21 SM code. Energy spectra and the angular distributions and ratios of the double differential protons and α particles were collected using the reaction ^{40}Ar + ^{27}Al at an incident laboratory energy of $E_{lab} = 190$ MeV. The α particle and proton energy spectra had not previously been reproduced with the single-step Monte Carlo approach, and in order to reproduce a subset of these, a very large deformation was assumed. The comparative analysis performed in this work was aimed at reproducing the full set of observables by taking advantage of the features of the LILITA_N21 evaporative code [14] in order to make our conclusion as solid as possible as well as to impose stringent constraints on the parameters characterizing CN decay. The LILITA_N21 code, which includes new Optical Model transmission coefficients, along with the multi-step Monte Carlo approach of the SM and a nuclear shape description based on the nuclear stratosphere provided an escape route from the previous impasse. A satisfactory reproduction of the complete set of observables was thereby obtained. In our calculation, we used: (i) a nuclear level density parameter, "a = A/8"; (ii) spherical nuclei with and without a small stratosphere volume; and (iii) transmission coefficients based on Optical Model potential parameters recently derived from global fits [27,28]. Concerning the OM parameterizations, it is worth noting that they include wide mass and energy ranges for emitting particles and a dependence on the difference between the neutron and proton

numbers that makes them well suited for calculations involving nuclei far from stability. Further improvements in SM ingredients, such as nuclear level density dependence on the isospin and nuclear temperature (as considered in [38]) and transmission coefficients, could be reached by simultaneously exploring evaporation residue yields and the neutron energy and angular distributions in the evaporative channels. Studies on this topic would greatly benefit of the measurement of γ rays and neutrons in coincidence with charged particles and evaporation residues and will be pursued in the near future, possibly by using the existing neutron detector array, e.g., NEDA [39,40] and adopting the approach described in [41] for measuring particle–γ ray coincidences.

Author Contributions: Investigation and Data curation, A.D.N., F.D. and E.V.; Supervision, E.V. and G.L.R.; Writing—original draft, A.D.N.; Writing—review & editing, E.V., D.B. and D.M. All authors have read and agreed to the published version of the manuscript.

Institutional Review Board Statement: Not applicable.

Informed Consent Statement: Not applicable.

Data Availability Statement: The data presented in this study are available within the article.

Conflicts of Interest: The authors declare no conflict of interest.

References

1. Weisskopf, V. Statistics and nuclear reactions. *Phys. Rev.* **1937**, *52*, 295–303. [CrossRef]
2. Weisskopf, V.F.; Ewing, D.H. On the yield of nuclear reactions with heavy elements. *Phys. Rev.* **1940**, *57*, 472–485. [CrossRef]
3. Feshbach, H. *Nuclear Spectroscopy, Part B*; Academic Press: New York, NY, USA, 1960; p. 625.
4. Vardaci, E.; Di Nitto, A.; Nadtochy, P.N.; La Rana, G. Fission dynamics in systems of intermediate fissility. *J. Phys. G Nucl. Part. Phys.* **2019**, *46*, 115111. [CrossRef]
5. Moro, R.; Brondi, A.; Gelli, N.; Barbui, M.; Boiano, A.; Cinausero, M.; Di Nitto, A.; Fabris, D.; Fioretto, E.; La Rana, G.; et al. Compound nucleus evaporative decay as a probe for the isospin dependence of the level density. *Eur. Phys. J. A* **2012**, *48*, 159. [CrossRef]
6. Di Nitto, A.; Vardaci, E.; Brondi, A.; La Rana, G.; Cinausero, M.; Gelli, N.; Moro, R.; Nadtochy, P.N.; Prete, G.; Vanzanella, A. Clustering effects in ^{48}Cr composite nuclei produced via the ^{24}Mg + ^{24}Mg reaction. *Phys. Rev. C* **2016**, *93*, 044602. [CrossRef]
7. Di Nitto, A.; Vardaci, E.; La Rana, G.; Nadtochy, P.N.; Boiano, A.; Cinausero, M.; Prete, G.; Gelli, N.; Kozulin, E.M.; Knyazheva, G.N.; et al. Evaporation and fission decay of ^{158}Er composite nuclei within the statistical model. *Phys. Rev. C* **2020**, *102*, 024624. [CrossRef]
8. Gonin, M.; Cooke, L.; Hagel, K.; Lou, Y.; Natowitz, J.B.; Schmitt, R.P.; Shlomo, S.; Srivastava, B.; Turmel, W.; Utsunomiya, H.; et al. Dynamical effects on the de-excitation of hot nuclei with A $\simeq$ 160. *Phys. Rev. C* **1990**, *42*, 2125–2142. [CrossRef]
9. Charity, R.J.; Sobotka, L.G.; Cibor, J.; Hagel, K.; Murray, M.; Natowitz, J.B.; Wada, R.; El Masri, Y.; Fabris, D.; Nebbia, G.; et al. Emission of unstable clusters from hot Yb compound nuclei. *Phys. Rev. C* **2001**, *63*, 024611. [CrossRef]
10. Vardaci, E.; Di Nitto, A.; Brondi, A.; La Rana, G.; Moro, R.; Nadtochy, P.N.; Trotta, M.; Ordine, A.; Boiano, A.; Cinausero, M.; et al. Inadequacy of the statistical model: Some evidence for compound nuclei in the A $\approx$ 150 and E$_x$ $\approx$ 100–200 MeV region. *Eur. Phys. J. A* **2010**, *43*, 127. [CrossRef]
11. La Rana, G.; Moro, R.; Brondi, A.; Cuzzocrea, P.; D'Onofrio, A.; Perillo, E.; Romano, M.; Terrasi, F.; Vardaci, E.; Dumont, H. Unexpected large deformations in ^{60}Ni nuclei produced in the reaction 120 MeV ^{30}Si + ^{30}Si. *Phys. Rev. C* **1988**, *37*, 1920. [CrossRef]
12. La Rana, G.; Moses, D.J.; Parker, W.E.; Kaplan, M.; Logan, D.; Lacey, R.; Alexander, J.M.; Welberry, R.J. Need for new physics in statistical models of nuclear de-excitation. *Phys. Rev. C* **1987**, *35*, 373. [CrossRef]
13. Batko, G.; Civitarese, O. Nuclear stratosphere formation and its effects upon statistical particle emission processes. *Phys. Rev. C* **1988**, *37*, 2647–2650. [CrossRef]
14. Davide, F.; Di Nitto, A.; Vardaci, E.; La Rana, G. LILITA_N21: Updated version of the Monte Carlo fusion–evaporation code. *Nucl. Instrum. Meth. Phys. Res. A* **2022**, *1025*, 166178. [CrossRef]
15. Hodgson, P.E. *Nuclear Heavy-Ion Reactions*; Clarendon Press: Oxford, UK, 1978; p. 588.
16. Pühlhofer, F. Computer code CASCADE. *Nucl. Phys. A* **1977**, *280*, 267. [CrossRef]
17. Reisdorf, W. Analysis of fissionability data at high excitation energies. *Z. Phys. A* **1981**, *300*, 227–238. [CrossRef]
18. Gavron, A. Statistical model calculations in heavy ion reactions. *Phys. Rev. C* **1980**, *21*, 230. [CrossRef]
19. Tarasov, O.; Bazin, D. LISE++: Radioactive beam production with in-flight separators. *Nucl. Instrum. Methods Phys. Res. Sect. B Beam Interact. Mater. At.* **2008**, *266*, 4657–4664. [CrossRef]
20. Gomez del Campo, J.; Stockstad, R.G. *Description and Use of the Monte Carlo Code LILITA [Modeling of Equilibrium Decay of Heavy Ion Reaction Products]*; Oak Ridge National Laboratory Report No. TM7295; Oak Ridge National Lab.: Oak Ridge, TN, USA, 1981.

21. Bohr, A.; Mottelson, B.R. *Nuclear Structure*; W. A. Benjamin: New York, NY, USA, 1969; Volume I, p. 152.

22. Fornal, B.; Gramegna, F.; Prete, G.; Burch, R.; D'Erasmo, G.; Fiore, E.M.; Fiore, L.; Pantaleo, A.; Paticchio, V.; Viesti, G.; et al. Level density of hot nuclei with A ⩽ 40. *Phys. Rev. C* **1991**, *44*, 2588–2597. [CrossRef]

23. Di Nitto, A.; Vardaci, E.; La Rana, G.; Nadtochy, P.N.; Prete, G. Evaporation channel as a tool to study fission dynamics. *Nucl. Phys. A* **2018**, *971*, 21–34. [CrossRef]

24. Huizenga, J.; Igo, G. Theoretical reaction cross sections for alpha particles with an optical model. *Nucl. Phys.* **1962**, *29*, 462–473. [CrossRef]

25. Perey, F.G. Optical-model analysis of proton elastic scattering in the range of 9 to 22 MeV. *Phys. Rev.* **1963**, *131*, 745–763. [CrossRef]

26. Wilmore, D.; Hodgson, P. The calculation of neutron cross-sections from optical potentials. *Nucl. Phys.* **1964**, *55*, 673–694. [CrossRef]

27. Köning, A.; Delaroche, J. Local and global nucleon optical models from 1 keV to 200 MeV. *Nucl. Phys. A* **2003**, *713*, 231–310. [CrossRef]

28. Su, X.W.; Han, Y.L. Global optical model potential for alpha projectile. *Int. J. Mod. Phys. E* **2015**, *24*, 1550092. [CrossRef]

29. Beck, C.; Papka, P.; Zafra, A.S.i.; Thummerer, S.; Azaiez, F.; Bednarczyk, P.; Courtin, S.; Curien, D.; Dorvaux, O.; Lebhertz, D.; et al. Binary reaction decays from ^{24}Mg + ^{12}C. *Phys. Rev. C* **2009**, *80*, 034604. [CrossRef]

30. Mahboub, D.; Beck, C.; Djerroud, B.; Freeman, R.M.; Haas, F.; Nouicer, R.; Rousseau, M.; Papka, P.; Sànchez iZafra, A.; Cavallaro, S.; et al. Light particle emission in ^{35}Cl + ^{24}Mg fusion reactions at high excitation energy and angular momentum. *Phys. Rev. C* **2004**, *69*, 034616. [CrossRef]

31. Rousseau, M.; Beck, C.; Bhattacharya, C.; Rauch, V.; Dorvaux, O.; Eddahbi, K.; Enaux, C.; Freeman, R.M.; Haas, F.; Mahboub, D.; et al. Highly deformed ^{40}Ca configurations in ^{28}Si + ^{12}C. *Phys. Rev. C* **2002**, *66*, 034612. [CrossRef]

32. Sierk, A.J. Macroscopic model of rotating nuclei. *Phys. Rev. C* **1986**, *33*, 2039. [CrossRef]

33. Cohen, S.; Plasil, F.; Swiatecki, W.J. Equilibrium configurations of rotating charged or gravitating liquid masses with surface tension. II. *Ann. Phys.* **1974**, *82*, 557–596. [CrossRef]

34. Vaz, L.C.; Alexander, J.M. Empirical and theoretical fusion barriers for1H and4He: Connections to evaporation from hot nuclei. *Z. Phys. A* **1984**, *318*, 231–237. [CrossRef]

35. Prajapati, G.K.; Gupta, Y.K.; John, B.V.; Joshi, B.N.; Kaur, H.; Kumar, N.; Danu, L.S.; Mukhopadhyay, S.; Dubey, S.; Jain, S.R.; et al. Temperature and isospin dependence of the level-density parameter in the $A \approx 110$ mass region. *Phys. Rev. C* **2020**, *102*, 054605. [CrossRef]

36. Roy, P.; Banerjee, K.; Rana, T.K.; Kundu, S.; Manna, S.; Sen, A.; Mondal, D.; Sadhukhan, J.; Senthil Kannan, M.T.; Ghosh, T.K.; et al. Evidence for the reduction of nuclear level density away from the β-stability line. *Phys. Rev. C* **2020**, *102*, 061601. [CrossRef]

37. Hüyük, T.; Di Nitto, A.; Jaworski, G.; Gadea, A.; Javier Valiente-Dobón, J.; Nyberg, J.; Palacz, M.; Söderström, P.A.; Jose Aliaga-Varea, R.; de Angelis, G.; et al. Conceptual design of the early implementation of the NEutron Detector Array (NEDA) with AGATA. *Eur. Phys. J. A* **2016**, *52*, 55. [CrossRef]

38. Di Nitto, A.; Brondi, A.; La Rana, G.; Moro, R.; Nadtochy, P.; Vardaci, E.; Gelli, N.; Cinausero, M.; Prete, G. The role of isospin in fusion evaporation reactions. *J. Phys. Conf. Ser.* **2011**, *267*, 012053. [CrossRef]

39. Modamio, V.; Valiente-Dobón, J.; Jaworski, G.; Hüyük, T.; Triossi, A.; Egea, J.; Di Nitto, A.; Söderström, P.A.; Agramunt Ros, J.; de Angelis, G.; et al. Digital pulse-timing technique for the neutron detector array NEDA. *Nucl. Instrum. Methods Phys. Res. Sect. A* **2015**, *775*, 71–76. [CrossRef]

40. Valiente-Dobón, J.; Jaworski, G.; Goasduff, A.; Egea, F.; Modamio, V.; Hüyük, T.; Triossi, A.; Jastrzab, M.; Söderström, P.; Di Nitto, A.; et al. NEDA—NEutron Detector Array. *Nucl. Instrum. Meth. Phys. Res. A* **2019**, *927*, 81–86. [CrossRef]

41. Vardaci, E.; Pulcini, A.; Kozulin, E.M.; Matea, I.; Verney, D.; Maj, A.; Schmitt, C.; Itkis, I.M.; Knyazheva, G.N.; Novikov, K.; et al. Using γ rays to disentangle fusion-fission and quasifission near the Coulomb barrier: A test of principle in the fusion-fission and quasielastic channels. *Phys. Rev. C* **2020**, *101*, 064612. [CrossRef]